

Optimization of out-of-plane magnetized Co/Pt multilayers with resistive buffer layers

Satoru Emori^{a)} and Geoffrey S. D. Beach

Department of Materials Science and Engineering, Massachusetts Institute of Technology, Cambridge, Massachusetts 02139, USA

(Received 1 March 2011; accepted 28 June 2011; published online 12 August 2011)

Ta oxide (TaOx) is investigated as a resistive buffer layer for the growth of high-quality Co/Pt multilayers with perpendicular magnetic anisotropy (PMA). The Pt/(Co/Pt)₃ films grown on TaOx buffer layers exhibit stronger PMA than those grown on Pt buffer layers, and are of comparable quality to films grown on metallic Ta. The optimized multilayers with TaOx buffer layers remain out-of-plane magnetized for Co layer thicknesses up to 10 Å without introducing a metallic current-shunting path, making these films attractive for spintronic devices using spin-polarized current. © 2011 American Institute of Physics. [doi:10.1063/1.3622613]

I. INTRODUCTION

A variety of proposed spintronic memory and logic devices¹ rely on electrical manipulation of the magnetization via spin-transfer torques.² Out-of-plane magnetized thin films have several key advantages over in-plane magnetized films for such device applications, including higher thermal stability,^{3–5} lower threshold currents for spin-transfer switching^{3,4} and current-induced domain wall motion.^{5–8} Maintaining out-of-plane magnetization in the remanent state requires perpendicular magnetic anisotropy (PMA) strong enough to overcome shape anisotropy and the consequent demagnetizing field. Strong PMA can be engineered in ultrathin multilayer (ML) films such as Co/Pt and Co/Pd stacks, with the Co layer thickness typically limited to a range of ~3–7 Å. The PMA in such MLs is usually attributed to asymmetries in interfacial bonding, crystallographic orientation, and/or magnetoelastic strain.^{9,10}

Recently, Co/Pt trilayers and MLs have been of particular interest as platforms for spin valves^{3,4,11} and studies of current-driven domain wall dynamics.^{12–16} However, current shunting by Pt and scattering at the Co/Pt interfaces decrease the spin polarization in Co/Pt-based devices,¹² thus reducing the giant magnetoresistance ratio^{3,11} and the efficiency of spin transfer torque.^{12–14} Moreover, high-quality Co/Pt ML growth usually requires one or more buffer layers to establish (111) crystallographic texture, which tends to enhance the PMA.^{17,18} These buffer layers are relatively thick (~20–200 Å) metallic underlayers such as Pt (Refs. 3, 4, and 11–18) and Ta (Refs. 3, 4, 14, 15, and 18) that aggravate the current-shunting problem.

To improve the performance of spintronic devices based on Co/Pt MLs, a larger fraction of current must be directed into the magnetic Co layers. Therefore, it is desirable to maximize the thickness of the Co layers wherein out-of-plane magnetization can be maintained, while minimizing current shunting by the buffer layers that promote film

quality and strong PMA. Although insulating underlayers have been utilized for in-plane magnetized spin valves,¹⁹ there have been no reports on the use of insulating buffer layers for out-of-plane magnetized Co/Pt MLs suitable for current-operated device applications. Here we investigate high-resistivity Ta oxide (TaOx) as an alternative to more common metal buffer layers for establishing high-quality out-of-plane magnetized Co/Pt MLs.

II. EXPERIMENTAL METHODS

The Co/Pt ML films were deposited on Si(100) substrates with a native SiO₂ overlayer by DC magnetron sputtering at a background pressure of ~8–10 × 10⁻⁸ Torr. The substrates were mounted on the perimeter of a rotating planetary table, sequentially passing over each shutter-controlled sputtering source with a period of 1.7 s. The configuration of the MLs from the substrate side was *buffer*/Pt(15)/[Co(*t*_{Co})/Pt(10)]₂/Co(*t*_{Co})/Pt(15), where the numbers in parentheses indicate the layer thickness in Å. A series of Co/Pt MLs with a Co layer thickness, *t*_{Co}, ranging from 6 to 12 Å was deposited on each of three buffer layers: Pt(120), Ta(30), and TaOx(30). The sputtering parameters for each material are listed in Table I. The TaOx buffer layers were deposited by reactive sputtering from a metallic Ta target with an O₂ partial pressure of ~6 × 10⁻⁵ Torr. After each TaOx deposition, reactive gas flow was terminated, followed by a pause of several minutes to allow the O₂ partial pressure to return to its background level before depositing subsequent layers. The resistivity of the TaOx film, measured using a standard four-point technique, was ~2.0 × 10⁻⁴ Ωm, which is about 2 orders magnitude greater than that of the Ta metal film at ~2.5 × 10⁻⁶ Ωm.

Magnetic characteristics were obtained from hysteresis loops measured perpendicular and parallel to the film plane using the magneto-optical Kerr effect (MOKE) in the polar and longitudinal configuration, respectively. The field sweep rate was 0.2 Hz.²⁰ X-ray diffraction (XRD) was used to

^{a)}Electronic mail: satorue@mit.edu.

TABLE I. Sputtering parameters.

	TaOx	Ta	Pt	Co
Deposition rate (Å/s)	0.65	0.43	0.27	0.18
Sputtering pressure (mTorr Ar)	2.0	2.0	3.0	3.0

correlate the crystallographic structure and film texture with the magnetic properties.

III. RESULTS AND DISCUSSION

Figure 1 shows the in-plane and out-of-plane hysteresis loops for MLs with $t_{Co} = 6$ Å deposited on each of the three buffer layers. All films exhibit square out-of-plane loops with a remanence ratio of $M_r/M_s \approx 1$, indicating dominant net PMA. The MLs deposited on the Ta metal and TaOx buffer layers have nearly identical hysteresis loops, with a coercivity of ~ 150 Oe and a hard-axis (in-plane) saturation field of ~ 4000 Oe. The ML with a Pt buffer layer has a much larger coercivity (~ 350 Oe), suggesting higher film quality with suppressed domain nucleation. However, the in-plane saturation field is actually slightly lower (~ 3200 Oe) for this sample, implying a weaker PMA.

To compare the influence of these buffer layers in detail, we have measured in-plane and out-of-plane hysteresis loops over a range of t_{Co} spanning the transition from perpendicular to in-plane anisotropy. A subset of these loops is shown in Fig. 2. The MLs grown on a Pt buffer layer maintain full out-

of-plane remanent magnetization up to $t_{Co} = 6$ Å, but at $t_{Co} = 7$ Å, the out-of-plane loop is sheared, and for $t_{Co} > 7$ Å, the MLs exhibit clear in-plane anisotropy. By contrast, MLs with Ta metal or TaOx buffer layers remain completely out-of-plane magnetized at remanence up to $t_{Co} = 10$ Å. Compared to Pt underlayers, both metallic Ta and resistive TaOx buffer layers increase the upper limit of t_{Co} by more than 50% for these Co/Pt MLs to exhibit out-of-plane magnetization.

The perpendicular anisotropy field, H_K , estimated from the hard-axis saturation field [in-plane loop for $H_k > 0$ and out-of-plane loop for $H_k < 0$ (see Ref. 21)], is plotted versus t_{Co} in Fig. 3(a). These data indicate that Ta metal and TaOx buffer layers produce MLs with nearly identical PMA, which is uniformly stronger than for MLs grown on Pt alone over this range of t_{Co} . The effective PMA energy density is defined as $K_{eff} = H_K M_S / 2$, where M_S is the saturation magnetization normalized by the Co volume. Here, the M_S was independently measured using a vibrating sample magnetometer (VSM). The results in Fig. 3(b) show that M_S in these Co/Pt MLs is significantly greater than the value measured for 41-nm-thick Co films at 1360 ± 30 emu/cm³. This enhancement of the magnetization in the Co/Pt MLs, which was also observed by Lin *et al.*,¹⁷ is likely due to the polarization of Pt at the Co/Pt interface. The magnitude of the M_S enhancement and the weak $1/t_{Co}$ dependence measured here agrees well with the results in Ref. 17, and suggests high-quality Co/Pt interfaces in these films.

In Fig. 3(c), we plot the product of t_{Co} and K_{eff} , using the mean saturation magnetization, $M_S = 1670 \pm 70$ emu/cm³ from the VSM data. This quantity, $K_{eff} t_{Co}$, may be interpreted in terms of phenomenological surface (K_S) and volume (K_V) contributions to the total PMA energy density,

$$K_{eff} t_{Co} = 2K_S + K_V t_{Co}. \quad (1)$$

For the MLs on Pt, and for those on Ta and TaOx with $t_{Co} \geq 10$ Å, the data follow a straight line with a slope consistent with a volume contribution dominated by the out-of-plane shape anisotropy energy, $K_V \approx -2\pi M_S^2 = -1.75 \times 10^7$ erg/cm³. By contrast, the data for the TaOx and Ta buffer samples at $t_{Co} \leq 10$ Å show a much weaker slope with t_{Co} , suggesting an additional positive volume-like contribution to K_{eff} that acts in a manner counter to the shape anisotropy. This additional K_V contribution is responsible for extending the range of t_{Co} over which net PMA is observed.

Figure 4 shows XRD spectra that give insight into the structural role of the buffer layers in enhancing PMA. The Co/Pt MLs with $t_{Co} = 7$ Å, grown on both Ta and TaOx buffer layers, show coherent Co/Pt (111) texture with a single (111) peak located between the bulk Co and Pt (111) peak positions, along with a weak superlattice side peak structure. The Ta-based buffer layers allow for smooth layer-by-layer (Frank–van der Merwe) growth of Pt and Co layers, which predominantly develop the thermodynamically favorable (111) orientation.⁶ The same ML grown on the thick Pt buffer layer, however, shows only a single broad peak near the Pt(111) bulk peak position, with a smaller peak area despite the much greater total Pt thickness in this film. The

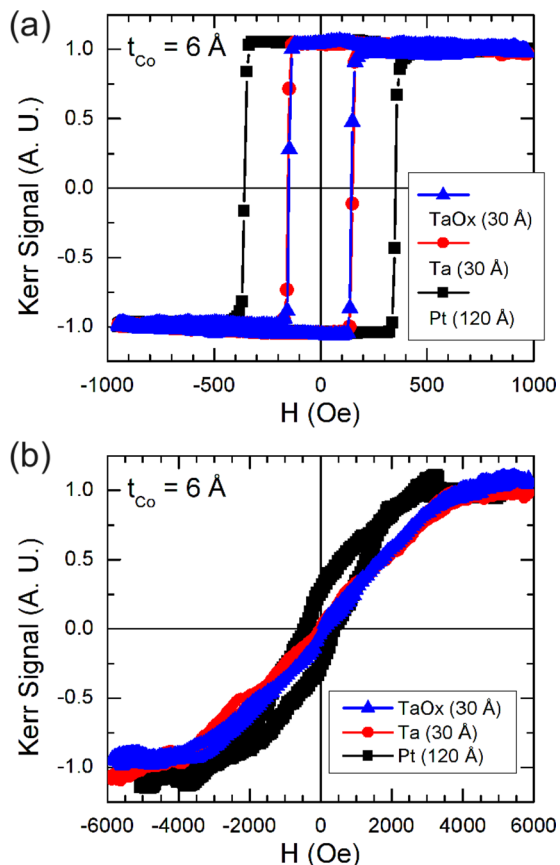


FIG. 1. (Color online) MOKE hysteresis loops of Co/Pt MLs with $t_{Co} = 6$ Å, obtained with (a) out-of-plane, and (b) in-plane magnetic fields.

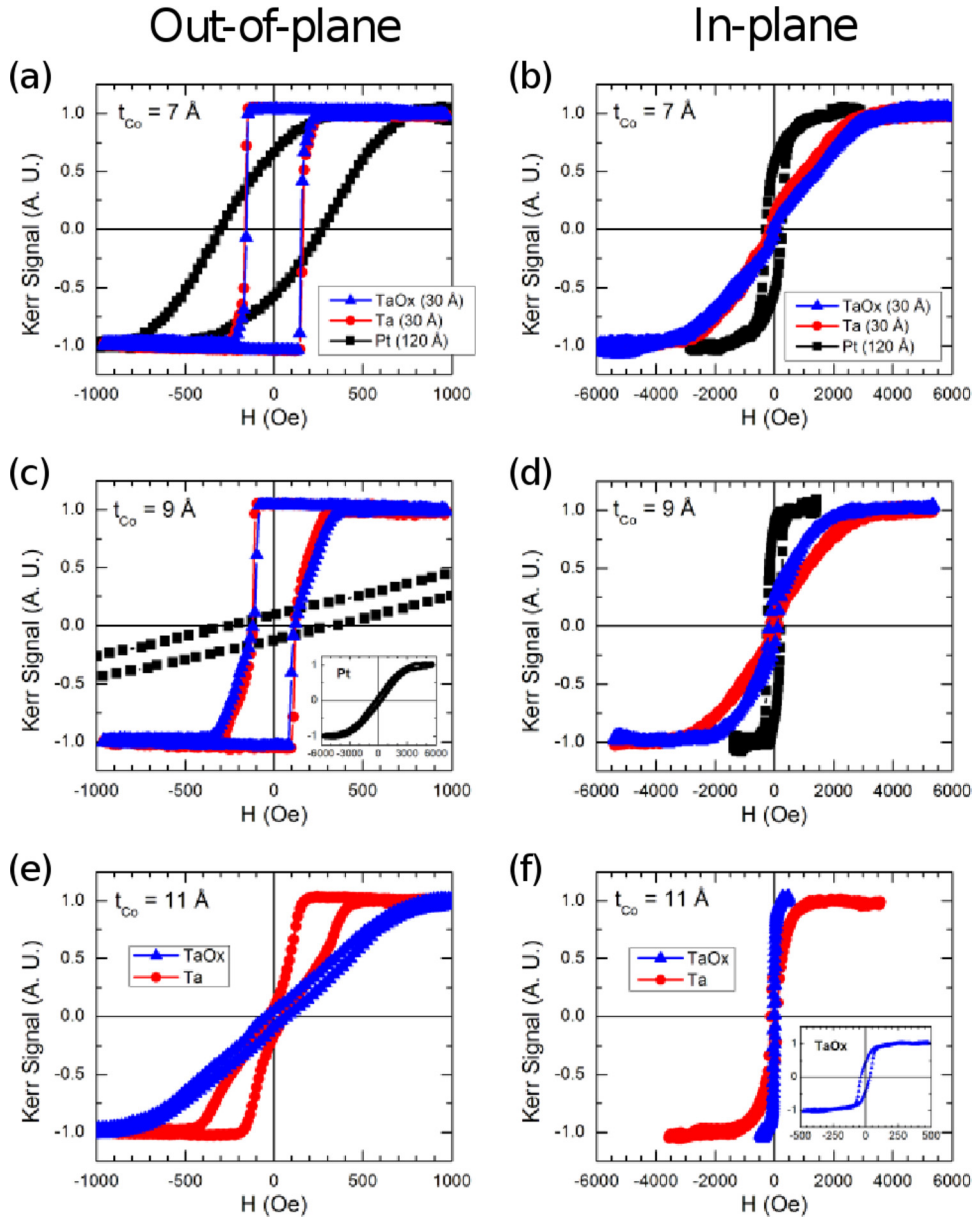


FIG. 2. (Color online) MOKE hysteresis loops of Co/Pt MLs with $t_{Co} = 7, 9,$ and 11 \AA , obtained with (a), (c), (e) out-of-plane, and (b), (d), (f) in-plane magnetic fields.

Coherent (111) texture in Co/Pt MLs is well known to be associated with strong PMA,^{17,18} through an increase in the magnetocrystalline anisotropy, K_{MC} , that may be oriented along the film normal and a magnetoelastic strain contribution, K_{ME} , that is due to the coherent growth of the lattice-mismatched Co and Pt layers.^{9,10} The combination of enhanced magnetocrystalline ($K_{MC} > 0$) and magnetoelastic ($K_{ME} > 0$) contributions thus offsets the shape anisotropy,

$$K_V = -2\pi M_S^2 + K_{MC} + K_{ME}. \quad (2)$$

From Fig. 4, Pt grown directly on the Si/SiO₂ surface does not develop significant (111) texture, but both Ta metal and TaOx are equally effective in promoting (111) texture in a Pt overlayer. The additional magnetocrystalline and strain contributions to PMA permit the Co/Pt MLs on the TaOx and Ta buffer layers to maintain out-of-plane remanent magnetization up to a larger t_{Co} of 10 Å. Beyond this layer

thickness, the coherent layer growth and strain can no longer be accommodated, and strain relaxation is expected.^{9,10} We speculate that for $t_{Co} > 10 \text{ \AA}$, the strain is relieved and the K_{ME} contribution to PMA is diminished, so K_V reflects only the shape anisotropy and remaining small K_{MC} component.

The preceding results show that a high-resistivity TaOx buffer layer is as effective as the commonly-used Ta metal buffer layers, and more effective than Pt alone, in promoting Co/Pt(111) texture and strong PMA. Having established TaOx as a viable alternative to metal buffer layers for Co/Pt growth, we determined the optimal TaOx thickness for maximizing PMA. Hysteresis loops of Co/Pt MLs with $t_{Co} = 9 \text{ \AA}$ and different TaOx buffer thicknesses (t_{TaOx}) were measured, and the estimated hard-axis anisotropy field H_k (\sim effective PMA energy density K_{eff}) is plotted against t_{TaOx} in Fig. 5. The PMA shows a maximum near $t_{TaOx} \approx 50 \text{ \AA}$. A thinner TaOx buffer layer ($t_{TaOx} < 30 \text{ \AA}$) may not be continuous, so

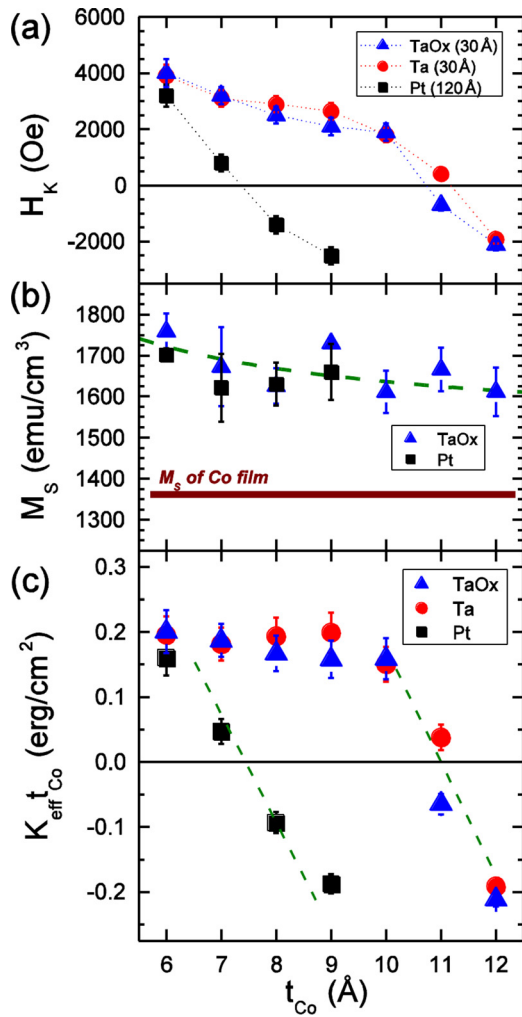


FIG. 3. (Color online) (a) Estimated anisotropy field H_K plotted against Co layer thickness, t_{Co} . (b) Saturation magnetization M_S plotted against t_{Co} . The dashed curve in the background is a guide for the eye. The solid horizontal line indicates the measured $M_S = 1360 \text{ emu/cm}^3$ of sputtered 41-nm-thick Co films. (c) Normalized effective PMA energy density, $K_{eff} t_{Co}$, plotted against t_{Co} . The MLs with $H_K > 0$ and $K_{eff} t_{Co} > 0$ are out-of-plane magnetized, and those with $H_K < 0$ and $K_{eff} t_{Co} < 0$ are in-plane magnetized. The dashed lines represent the shape anisotropy energy density, $-2\pi M_S^2 = -1.75 \times 10^7 \text{ erg/cm}^3$.

the Co/Pt ML grown on top of it may be of poor quality and have weaker PMA. On the contrary, if TaOx is too thick ($t_{TaOx} > 50 \text{ Å}$), the increased roughness may contribute to a reduction in structural quality and PMA.

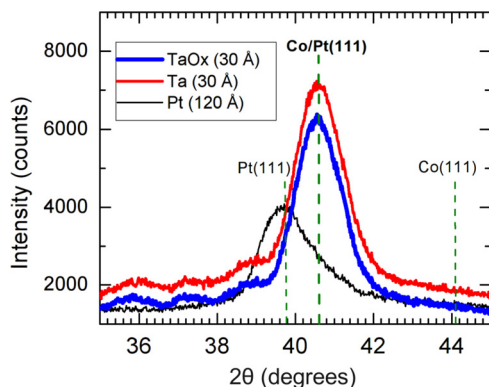


FIG. 4. (Color online) XRD spectra of $t_{Co} = 7 \text{ Å}$ Co/Pt MLs.

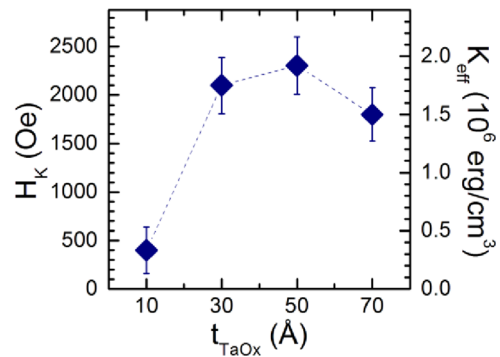


FIG. 5. (Color online) Estimated anisotropy field, H_K , and effective PMA energy density, K_{eff} , vs TaOx buffer thickness, t_{TaOx} .

IV. SUMMARY

We have characterized the viability of TaOx as a buffer layer for producing high-quality Co/Pt MLs with enhanced PMA. The MLs sputtered on TaOx buffer layers exhibit PMA comparable to MLs on metallic Ta buffer layers, and superior to MLs on Pt buffer layers. In particular, TaOx buffer layers allow Co/Pt to maintain remanent out-of-plane magnetization up to $t_{Co} = 10 \text{ Å}$, which is a significant increase compared to the upper limit of $t_{Co} = 6 \text{ Å}$ attained with Pt buffer layers. The enhancement of PMA by using TaOx buffer layers is attributed to smooth layer growth with pronounced (111) crystallographic orientation and coherent strain at $t_{Co} \leq 10 \text{ Å}$. The use of resistive TaOx eliminates the conductive current shunt path through the buffer layer and increases the maximum t_{Co} at which the ML remains out-of-plane magnetized. Compared to conventional Co/Pt ML stacks, we expect the current spin polarization and the performance of current-driven magnetic memory devices to be improved in these optimized TaOx/Pt(Co/Pt)₃ films.

ACKNOWLEDGMENTS

S.E. acknowledges David Bono, Stephen Salinas, and Uwe Bauer for their technical assistance, and the National Science Foundation Graduate Research Fellowship Program for financial support. The X-Ray Diffraction Shared Experimental Facility in the MIT Center for Materials Science and Engineering was used to characterize thin films in this study.

- ¹C. Chappert, A. Fert, and F. N. Van Dau, *Nature Mater.* **6**, 813 (2007).
- ²D. C. Ralph and M. D. Stiles, *J. Magn. Magn. Mater.* **320**, 1190 (2008).
- ³S. Mangin, D. Ravelosona, J. A. Katine, M. J. Carey, B. D. Terris, and E. E. Fullerton, *Nature Mater.* **5**, 210 (2006).
- ⁴S. Mangin, Y. Henry, D. Ravelosona, J. A. Katine, and E. E. Fullerton, *Appl. Phys. Lett.* **94**, 012502 (2009).
- ⁵S. Fukami, T. Suzuki, K. Nagahara, N. Ohshima, and N. Ishiwata, *J. Appl. Phys.* **108**, 113914 (2010).
- ⁶S. Fukami, T. Suzuki, H. Tanigawa, N. Ohshima, and N. Ishiwata, *Appl. Phys. Express* **3**, 113002 (2010).
- ⁷S. Fukami, T. Suzuki, N. Ohshima, K. Nagahara, and N. Ishiwata, *J. Appl. Phys.* **103**, 07E718 (2008).
- ⁸S.-W. Jung, W. Kim, T.-D. Lee, K.-J. Lee, and H.-W. Lee, *Appl. Phys. Lett.* **92**, 202508 (2008).
- ⁹M. T. Johnson, P. J. H. Bloemen, F. J. A. den Broeder, and J. J. de Vries, *Rep. Prog. Phys.* **59**, 1409 (1996).
- ¹⁰B. Zhang, K. M. Krishnan, C. H. Lee, and R. F. C. Farrow, *J. Appl. Phys.* **73**, 6198 (1993).

- ¹¹F. Garcia, F. Fettar, S. Auffret, B. Rodmacq, and B. Dieny, *J. Appl. Phys.* **93**, 8397 (2003).
- ¹²M. Cormier, A. Mougín, J. Ferré, A. Thiaville, N. Charpentier, F. Piéchon, R. Weil, V. Baltz, and B. Rodmacq, *Phys. Rev. B* **81**, 024407 (2010).
- ¹³T. A. Moore, I. M. Miron, G. Gaudin, G. Serret, S. Auffret, B. Rodmacq, A. Schuhl, S. Pizzini, J. Vogel, and M. Bonfim, *Appl. Phys. Lett.* **93**, 262504 (2008).
- ¹⁴T. Suzuki, S. Fukami, K. Nagahara, N. Ohshima, and N. Ishiwata, *IEEE Trans. Magn.* **44**, 2535 (2008).
- ¹⁵K.-J. Kim, J.-C. Lee, S.-J. Yun, G.-H. Gim, K.-S. Lee, S.-B. Choe, and K.-H. Shin, *Appl. Phys. Express* **3**, 083001 (2010).
- ¹⁶D. Ravelosona, D. Lacour, J. A. Katine, B. D. Terris, and C. Chappert, *Phys. Rev. Lett.* **95**, 117203 (2005).
- ¹⁷C.-J. Lin, G. L. Gorman, C. H. Lee, R. F. C. Farrow, E. E. Marinero, H. V. Do, H. Notarys, and C. J. Chien, *J. Magn. Magn. Mater.* **93**, 194 (1991).
- ¹⁸J. Kanak, M. Czapkiewicz, T. Stobiecki, M. Kachel, I. Sveklo, A. Maziewski, and S. van Dijken, *Phys. Status Solidi A* **204**, 3950 (2007).
- ¹⁹S. Maat, M. J. Carey, E. E. Fullerton, T. X. Le, P. M. Rice, and B. A. Gurney, *Appl. Phys. Lett.* **81**, 520 (2002).
- ²⁰For films with strong PMA whose coercivities can vary significantly with the field sweep rate, the out-of-plane field was swept at a fixed rate of ~ 800 Oe/s.
- ²¹In cases where the remanent magnetization in either direction was small (i.e., the magnetic anisotropy was close to the transition between in-plane and out-of-plane), H_K was estimated from the difference between the saturation fields in the in-plane and out-of-plane directions.